

Towards Understanding *Trans*-Cleavage of Natural and Synthetic Nucleic Acids by Cas12a for Sensitive CRISPR Biosensing

Fei Deng^{a,b,*}, Rui Sang^{a,b}, Yi Li^{a,b}, Danting Yang^c, Wei Deng^d, Ewa M. Goldys^{a,b,*}

^a Graduate School of Biomedical Engineering, Faculty of Engineering, University of New South Wales, Sydney 2052, Australia

^b ARC Centre of Excellence for Nanoscale Biophotonics, University of New South Wales, Sydney 2052, Australia

^c School of Public Health, Zhejiang Key Laboratory of Pathophysiology, Health Science Center, Ningbo University, Ningbo 315211, China

^d School of Biomedical Engineering, University of Technology Sydney, Sydney, NSW, 2007, Australia

* Correspondence: e.goldys@unsw.edu.au; fei.deng@unsw.edu.au

Abstract

CRISPR/Cas systems have been widely utilized for the development of biosensing platforms for precision molecular diagnostics. Their remarkable biosensing performance critically depends on the efficiency of sequence-independent *trans*-cleavage in type V and VI Cas effectors. Cas12a, a typical example of type V Cas effector exhibits varying *trans*-cleavage efficiency on different types of nucleic acids, and also in response to different nucleobase sequences. However, the underlying mechanism of Cas12a's *trans*-cleavage characteristic remains unclear. To explore this mechanism, we introduced Xeno nucleic acids (XNA) as potential *trans*-cleavage substrates of Cas12a. XNAs are chemically modified nucleic acid analogues, which originate from chemical modifications of nucleobases, sugar moieties, and the backbone. We observed a progressive decrease in *trans*-cleavage rates by Cas12a across different types of XNAs, in the following sequence: nucleobase-modified XNA > sugar moiety-modified XNA > backbone-modified XNA. In addition, more complex chemical modifications on either of the three above locations led to the lowering of the *trans*-cleavage rate of Cas12a. These findings elucidate the mechanism behind Cas12a's *trans*-cleavage characteristic, which is attributed to varying molecular complexity of the sugar moieties and nucleobases. Based on these findings, we also developed a colorimetric CRISPR/Cas12a biosensing system utilizing XNA for the detection of circulating tumor DNA (ctDNA), with a

limit of detection of 10 pM and a 4 logs detection range from 10 pM to 100 nM. These results indicate that XNA can serve as a novel Cas12a *trans*-cleavage target for sensitive biosensing applications.

Key words

CRISPR/Cas12a, *trans*-cleavage, Xeno nucleic acid, colorimetric biosensing

Highlights

1. XNAs represent alternative *trans*-cleavage substrates for Cas12a.
2. Cas12a demonstrates varying XNA *trans*-cleavage rates in the following order: nucleobase modified XNA > sugar moieties modified XNA > backbone modified XNA.
3. More complex chemical modifications on nucleobases, sugar moieties or backbone lead to a more pronounced lowering of Cas12a *trans*-cleavage rates.
4. The biosensing performance of the CRISPR/Cas12a systems based on XNA is comparable to that of equivalent conventional DNA-based systems.

Introduction

Programmable CRISPR/Cas systems, which have evolved as part of prokaryotic immunity, are capable of recognizing target nucleic acids, as well as exhibiting precise sequence-dependent (*cis*) and sequence-independent (*trans*) cleavage properties^{1,2}. The latter found extensive utility for the detection of various types of molecular targets, including nucleic acids^{2, 3}, small proteins^{4,5} and microorganisms⁶. The integration of CRISPR/Cas nucleases with conventional nucleic acid amplification technologies has led to the development of first CRISPR biosensing systems, such as DETECTR system (comprising recombinase polymerase amplification (RPA) followed by Cas12a readout)⁷, SHERLOCK system (comprising RT-RPA with Cas13 readout)⁸, and HOLMES (comprising PCR with Cas12a readout)⁹. In these and other CRISPR/Cas biosensing systems, the *trans*-cleavage ability of type V (e.g. Cas12 and Cas14)

and type VI (e.g. Cas13) Cas Ribonucleoproteins (RNPs) plays a key role in signal amplification^{2,5}.

Cas12a, also known as Cpf1, is a type V Cas effector with higher *trans*-cleavage rate on single strand DNA (ssDNA)¹⁰, than on double strand DNA (dsDNA)¹¹ and single strand RNA (ssRNA)^{12,13}. Furthermore, within the single-stranded DNA target category, Cas12a exhibits varying *trans*-cleavage rates depending on the nucleobase sequences (C > T > A > G)^{14,15}. However, the underlying mechanism of Cas12a's *trans*-cleavage characteristic remains unclear. To clarify the potential mechanism, Xeno nucleic acids (XNAs) with adjustable chemical properties^{16,17} were introduced as the *trans*-cleavage substrate of Cas12a.

XNA, a category of chemically altered nucleic acid analogues, possesses distinct properties from those of natural DNA and RNA, thereby offering novel possibilities across various applications¹⁶. The chemical modifications of nucleic acids to generate XNAs can be introduced at the level of nucleobases, the sugar moieties, and/or phosphodiester backbone. Such modifications yield a spectrum of effects. For example, altering nucleobases can influence base-pairing strength and its specificity, while adjustments to the phosphodiester backbone can increase resistance against nucleases and improve pharmacokinetic characteristics¹⁸. Furthermore, modifications to the sugar moieties exert a substantial impact on a range of nucleic acid properties, including the ability to form duplexes, nuclease resistance, and biocompatibility in both cellular and animal studies¹⁸. To date, XNA has been widely used for biomedical applications, such as in XNA-based aptamers, and XNAzymes¹⁷. XNA has also been used for the modifications of gRNA in CRISPR/Cas systems for gene editing; these included phosphorothioate modified gRNA¹⁹, 2'-O-Methyl modified gRNA²⁰ and diverse terminal chemical modifications²¹. As of now, there have been no investigations assessing the *trans*-cleavage rates of Cas12a on XNA to explore the potential mechanism of Cas12a's *trans*-cleavage preferences.

In this study, we designed three types of linear XNAs to be used as *trans*-cleavage targets of Cas12a (Fig. 1). These short (5nt) XNA linear sequences were modified with Texas Red on the 5' end, and BHQ2 on the 3' end, as standard fluorescent reporters. Subsequently, their *trans*-cleavage performance was evaluated in a basic CRISPR/Cas12 biosensing system (Fig. 1), and the results were analysed from the perspective of chemical structures. We analysed the *trans*-cleavage rates of Cas12a across different types of XNAs and found that the mechanism behind Cas12a' *trans*-cleavage preferences is due to varying molecular complexity of the sugar moieties and nucleobases. Based on these findings, we also developed a colorimetric CRISPR/Cas12a biosensing system utilizing deoxyUridine (dU) based XNA reporters for the detection of circulating tumor DNA (ctDNA). The system achieved the limit of detection of 10 pM with 4 log detection range (10 pM to 100 nM), which is sufficient for the testing of ctDNA in biological samples in clinical conditions.²² Collectively, our results show that dU-XNA based colorimetric reporters provide an effective approach for the development of CRISPR/Cas biosensing system for testing of nucleic acid targets.

Materials and Methods

1. Materials and reagents

Biological reagents: EnGen® Lba Cas12a (Cpf1) protein (New England Biolab), 10X NEB 2.1 buffer (New England Biolab), DNase/RNase free water (ThermoFisher), phosphate buffered saline (PBS) (Sigma, 10 mM, pH=7.4), Dithiothreitol (DTT) (Sigma, DTT-RO), SigmaFast OPD (P9187), Magnetic beads (Spherotech, SVM-08-10), and HRP Anti-Fluorescein antibody (abcam, ab6656).

Oligos: All designed RNA and DNA oligos were synthesized by Sangon Biotech.

Table 1. DNA and RNA oligos used in this study.

Name	Oligo type	Sequence 5'-3'	Modification
gRNA	ssRNA	UAA UUU CUA CUA AGU GUA GAU GAC AUA GCA CAU AGA CUG AGA	N/A

Trigger	ssDNA	TCT CAG TCT ATG TGC TAT GTC	N/A
5A substrate	ssDNA	AAAAA	5'-Texas Red; 3'-BHQ2
5T substrate	ssDNA	TTTTT	5'-Texas Red; 3'-BHQ2
5C substrate	ssDNA	CCCCC	5'-Texas Red; 3'-BHQ2
5G substrate	ssDNA	GGGGG	5'-Texas Red; 3'-BHQ2
DNA substrate	ssDNA	TTATT	5'-Texas Red; 3'-BHQ2
DNA-rA substrate	DNA-RNA	TT/rA/TT	5'-Texas Red; 3'-BHQ2
RNA substrate	ssRNA	UUAUU	5'-Texas Red; 3'-BHQ2
Beta-L-DNA substrate	DNA-beta-L- DNA	TT/beta-L-A/TT	5'-Texas Red; 3'-BHQ2
deoxyUridine (dU) substrate	DNA- deoxyUridine	TT/deoxyUridine/TT	5'-Texas Red; 3'-BHQ2
5-Aza-2'- deoxycytidine substrate	DNA-5-Aza-2'- deoxycytidine	TT/5-Aza-2'-deoxycytidine/TT	5'-Texas Red; 3'-BHQ2
5-Nitroindole substrate	DNA-5- Nitroindole	TT/5-Nitroindole/TT	5'-Texas Red; 3'-BHQ2
2-Aminopurine substrate	DNA-2- Aminopurine	TT/2-Aminopurine/TT	5'-Texas Red; 3'-BHQ2
Phosphorothioate substrate	DNA	TT*A*TT	5'-Texas Red; 3'-BHQ2
Azobenzene substrate	DNA	TT*A*TT	5'-Texas Red; 3'-BHQ2
2F-RNA substrate	DNA-2F-RNA	TT/2F-RNA/TT	5'-Texas Red; 3'-BHQ2
2'-O-Methyl substrate	DNA-2'-O- Methyl	TT/2'-O-Methyl/TT	5'-Texas Red; 3'-BHQ2
2-methoxyethyl substrate	DNA-2- methoxyethyl	TT/2-methoxyethyl/TT	5'-Texas Red; 3'-BHQ2
LNA	DNA-LNA	TT/LNA/TT	5'-Texas Red; 3'-BHQ2
dU XNA linker	XNA	TT/dU/TTTT/dU/TTTT/dU/TT	3'-Biotin; 5'- FAM
ct-gRNA	ssRNA	UAA UUU CUA CUA AGU GUA GAU CCU CUC UCU AAA AUC ACU GAG	N/A
ctDNA	ssDNA	CTC AGT GAT TTT AGA GAG AGG AT	N/A

2. Investigating the *trans*-cleavage ability of Cas12a on XNA substrate

A standard CRISPR/Cas12a reaction solution was prepared as follows. In brief, 10 μL of 10 μM Cas12a protein, 5 μL of 20 μM gRNA, and 6 μL of 100 μM XNA substrate were added into 1X 3.6 mL NEB2.1 buffer. The prepared solution was stored in 4 $^{\circ}\text{C}$ before use. Afterwards, 5 μL of 1 μM trigger ssDNA was added to 100 μL of prepared CRISPR/Cas reaction mixture to trigger the reaction and incubated at room temperature for two hours. An ID3 plate reader was applied for the detection of fluorescence readout with excitation wavelength of 570 nm and emission wavelength of 615 nm.

3. Synthesis and optimization of magnetic beads-dU-XNA-HRP reporter.

Firstly, 20 μL of 0.5% w/v streptavidin modified magnetic beads (0.74 μm) was washed twice with PBS buffer. Subsequently, 100 μL of a range of biotin-dU-XNA-FAM solution (0, 0.5, 1, 2, 4 μM XNA in 1% BSA solution) was mixed with magnetic beads for 30 min at room temperature, and free biotin-dU-XNA-FAM was removed by PBS wash. After formation of the magnetic beads-dU-XNA conjugate, HRP labelled anti-FAM antibody was introduced to form the magnetic beads-dU-XNA-HRP conjugation. A range of anti-FAM antibody concentrations were tested (0, 1.25, 2.5, 5, 10, 20 $\mu\text{g}/\text{mL}$), and the free antibody was removed by PBS wash. The final magnetic beads-dU-XNA-HRP reporter was added in 100 μL OPD solution. After incubation for 10 min, the absorbance value was detected using ID3 plate reader at 492 nm.

4. Biosensing application of dU-XNA reporter based CRISPR/Cas12a biosensing system

A CRISPR/Cas12a reaction mixture was prepared as follows: 10 μL 10 μM (100 pmol) of Cas12a protein was gently mixed with 5 μL 20 μM (100 pmol) of ct-gRNA, 36 μL of 1 M DTT and 72 μL of HRP labelled dU-XNA reporter (1%) in a total of 3.6 mL 1X NEB 2.1 buffer. A range of target synthetic DNA sequences (ctDNA in Table 1) (0, 10 pM, 100 pM, 1 nM, 10 nM, 100 nM) was applied in 100 μL of prepared CRISPR/Cas reaction mixture for starting the CRISPR reaction process. After incubation for 60 min at 37 $^{\circ}\text{C}$, magnetic separation was applied, and the supernatant was removed. Subsequently, 100 μL OPD solution was added, and incubated for 10 min. The absorbance value was detected using ID3 plate reader at 492 nm.

Results

1. XNA design and characterization

Natural nucleic acids comprise nucleobases, sugar moieties and the phosphodiester backbone. In this study corresponding chemical modifications have been made on each of these three components. As shown in Fig. 1A, natural nucleobase contains A, T, C, G, U, have been replaced by synthetic nucleobases, including deoxyUridine, 5-Aza-2'-deoxycytidine, 5-Nitroindole, and 2-Aminopurine. Natural sugar moieties H (DNA) and OH (RNA), have been replaced by synthetic sugar moieties, including 2F-RNA, 2'-O-Methyl, 2-methoxyethyl, and LNA. The natural backbone is a phosphodiester, which has been replaced here by beta-L-DNA, phosphorothioate, or azobenzene.

To characterize the *trans*-cleavage characteristic of Cas12a on different types of XNA substrates, we established a fluorescent assay using these nucleic acid structures as fluorescent reporters. As shown in Fig. 1B, after mixing the trigger DNA with Cas12a RNP, the *trans*-cleavage activity of Cas12a RNP is activated, which then cleaves the fluorescent XNA reporters allowing them to release the Texas Red fluorophore from the BHQ2 quencher for fluorescent signal readout.

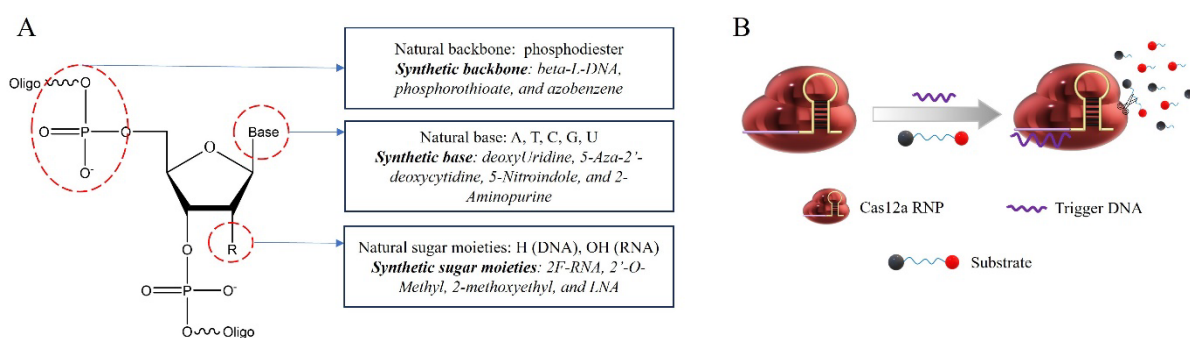


Figure 1. Schematics of XNA design and characterization. (A) Chemical modification of nucleic acids on their bases, sugar moieties, and the backbone to generate XNAs; (B) Schematic diagram of a basic CRISPR/Cas12a sensor utilized to characterize the Cas12a's *trans*-cleavage efficiency on XNA based substrates.

2. Exploration of the *trans*-cleavage ability of Cas12a on nucleobase-modified XNA target.

In this section, we investigate the *trans*-cleavage ability of Cas12a on natural and synthetic nucleobase sequences (Fig. 2). In terms of natural nucleobase sequences (Fig. 2A), the Cas12a *trans*-cleavage rates of Pyrimidine sequences (C and T) were higher than that of Purine (A and G), since the molecular structure of single ring Pyrimidine was simpler than that of two rings Purine. This finding was further verified by synthetic nucleobase sequences. As shown in Fig. 2C, the *trans*-cleavage rates of single-ring nucleobases (deoxyUridine (dU) and 5-Aza-2'-deoxycytidine) by Cas12a were higher than those of two-ring nucleobases (5-Nitroindole and 2-Aminopurine). Therefore, more complex molecular structure of nucleobase tends to restrict the *trans*-cleavage activity of Cas12a.

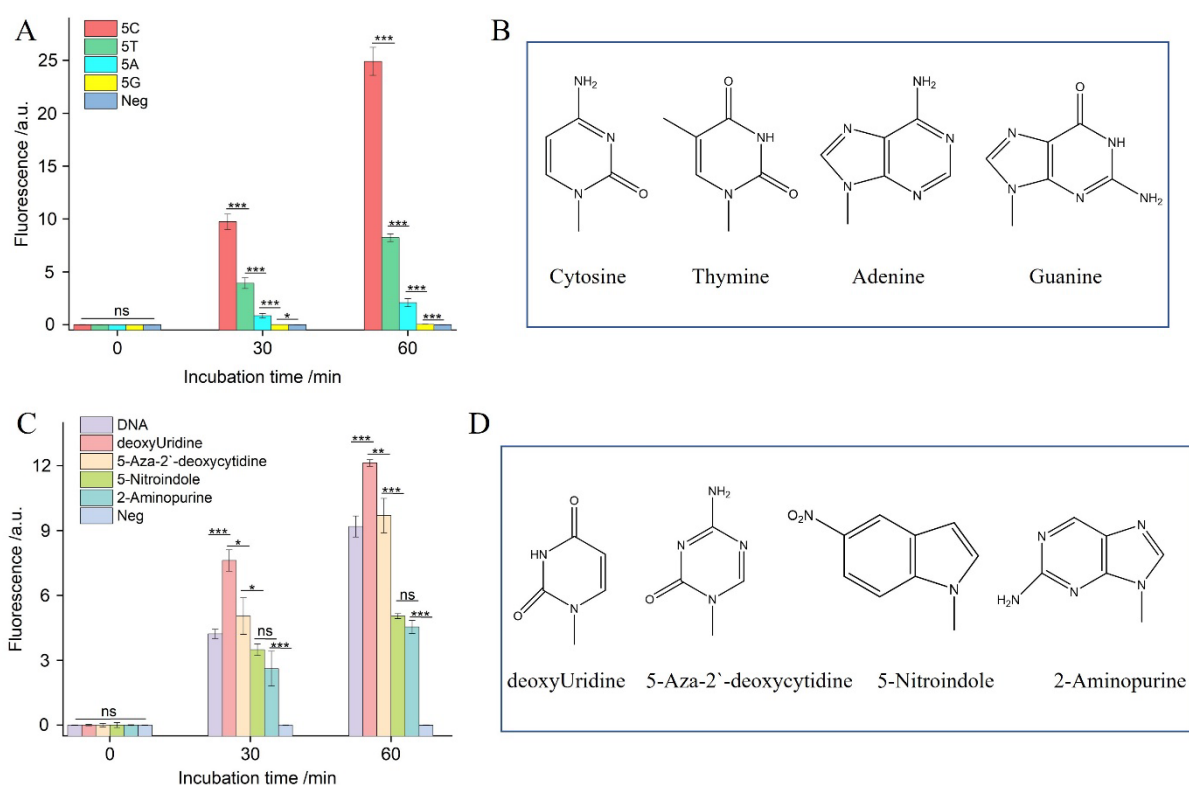


Figure 2. Exploring the *trans*-cleavage ability of Cas12a on nucleobase-modified XNA target. (A) *trans*-cleavage performance of Cas12a on diverse natural nucleobase sequence (n=3); (B)

Chemical structures of natural nucleobases; (C) *trans*-cleavage performance of Cas12a on diverse synthetic nucleobase sequence (n=3); (D) Chemical structures of synthetic nucleobases. (* P<0.05, ** P<0.01, *** P<0.005, ns = not significant)

3. Investigation of the *trans*-cleavage ability of Cas12a on sugar moiety-modified XNA target.

In this section, we investigate various types of nucleic acids featuring different sugar moieties (Fig. 3), including H (DNA), OH (RNA), 2F-RNA, 2'-O-Methyl, 2-methoxyethyl, and LNA. In terms of natural nucleic acids (Fig. 3A), the Cas12a *trans*-cleavage rates follow the sequence of DNA > DNA-RNA > RNA, which is aligned with differences of sugar moieties in DNA (H), and RNA (OH). In order to further explore the *trans*-cleavage preferences of Cas12a, new synthetic sugar moieties were introduced. As shown in Fig. 3B, with the introduction of different synthetic sugar moieties, the fluorescence signals exhibited a decreasing order: DNA > 2F-RNA > 2'-O-Methyl > 2-methoxyethyl > LNA, which is consistent with the corresponding trends in molecular complexity (Fig. 3C). Therefore, with the increase of molecular complexity in sugar moieties, the XNA becomes more and more resilient to *trans*-cleavage by Cas12a.

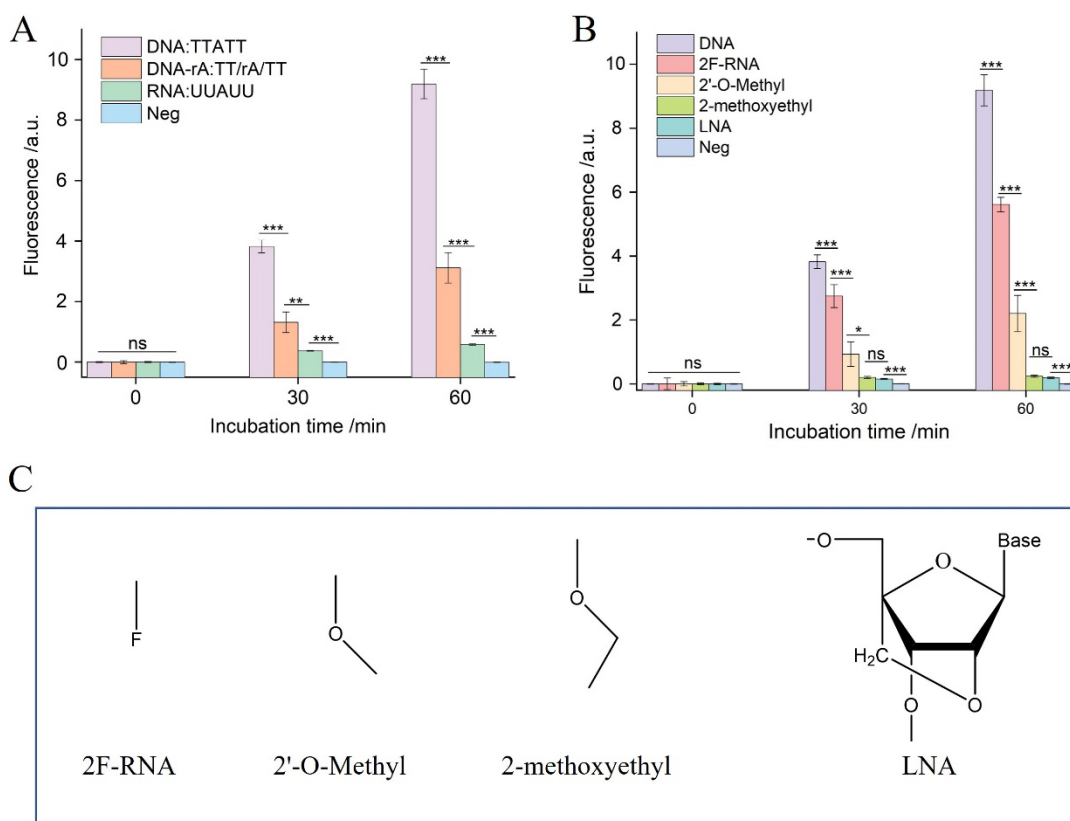


Figure 3. Exploring the *trans*-cleavage ability of Cas12a on sugar moiety modified XNA target. (A) *trans*-cleavage performance of Cas12a on natural nucleic acids (Method 2, n=3); (B) *trans*-cleavage performance of Cas12a on diverse sugar moieties modified XNA targets (n=3); (C) Chemical structures of diverse sugar moieties. (* P<0.05, ** P<0.01, *** P<0.005, ns = not significant)

4. Investigation of the *trans*-cleavage ability of Cas12a on phosphodiester backbone-modified XNA target.

In this section, we investigate the chemical modification on the phosphodiester backbone, including beta-L-DNA, phosphorothioate, and azobenzene (Fig. 4A). As shown in Fig. 4B, limited fluorescence increases were observed in all three backbone-modified XNAs, indicating that chemical modification on the backbone significantly restricted the *trans*-cleavage rates of Cas12a, which is unsurprising since Cas12a is an endonuclease which cleaves the

phosphodiester backbone⁹. We also explored Beta-L-DNA which is the mirror image version of naturally occurring D-DNA²³. Limited fluorescence increase was observed in beta-L-DNA compared with D-DNA, indicating that chemical structure conformation influences the *trans*-cleavage rate of Cas12a. In addition, the fluorescence signal of phosphorothioate-modified XNA was higher than that of azobenzene modified XNA (Fig. 4B), which is consistent with the trend of higher molecular complexity (Fig. 4C). These data indicate that more complex chemical modifications of the phosphodiester backbone lead to a lower *trans*-cleavage rate of Cas12a.

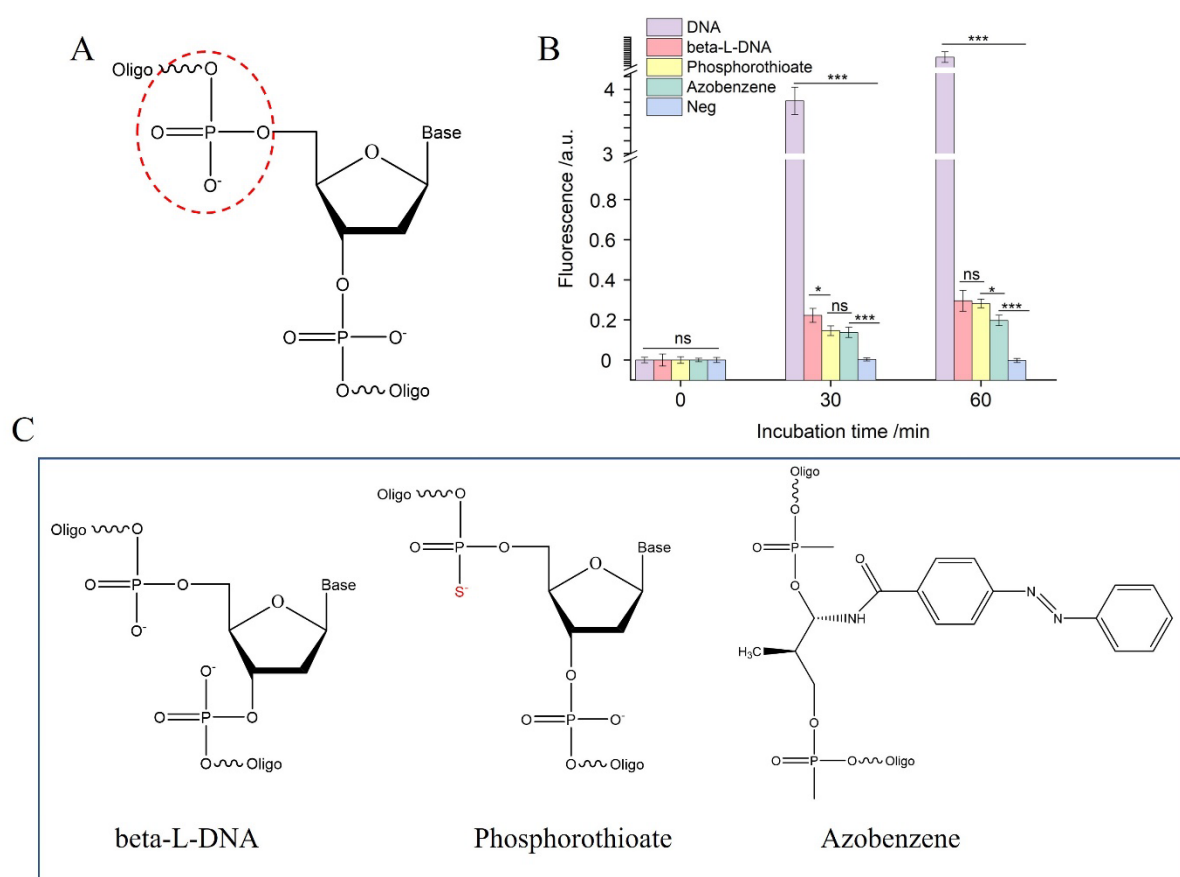


Figure 4. Exploring the *trans*-cleavage of Cas12a on phosphodiester backbone modified XNA target. (A) The location of phosphodiester backbone on nucleic acids; (B) *trans*-cleavage performance of Cas12a on different phosphodiester backbone-modified XNA targets (n=3); (C)

Chemical structures of phosphodiester backbone modified XNAs. (* P<0.05, ** P<0.01, *** P<0.005, ns = not significant)

5. Application of dU-XNA reporter based CRISPR/Cas12a biosensing system for the detection of ctDNA

To develop an XNA-based colorimetric biosensing system, dU was selected since it shows high *trans*-cleavage rate on ssDNA (Fig. 2C). The colorimetric magnetic bead-XNA-HRP (MB-XNA-HRP) reporter was synthesized by immobilising XNA on the surface of magnetic beads followed by the attachment of HRP on top of XNA (Fig. 5A). Each component was optimized (Fig.5B&C&S1). The schematic of the MB-XNA-HRP reporter-based CRISPR/Cas12a biosensing system is shown in Fig. 5D. The system operates as follows. After the addition of the DNA target, the *trans*-cleavage of Cas12a RNP is activated, which non-specifically cleaves the XNA linker in the MB-XNA-HRP reporter to release the HRP protein. The remaining HRP on the MB-XNA-HRP reporter is then able to react with a suitable colorimetric substrate (OPD) for signal readout. This MB-XNA-HRP reporter-based CRISPR/Cas12a biosensing system was applied for the detection of short synthetic DNA sequences. As shown in Fig. 5E, the limit of detection was determined to be 10 pM with a 4-log detection range from 10 pM to 100 nM.

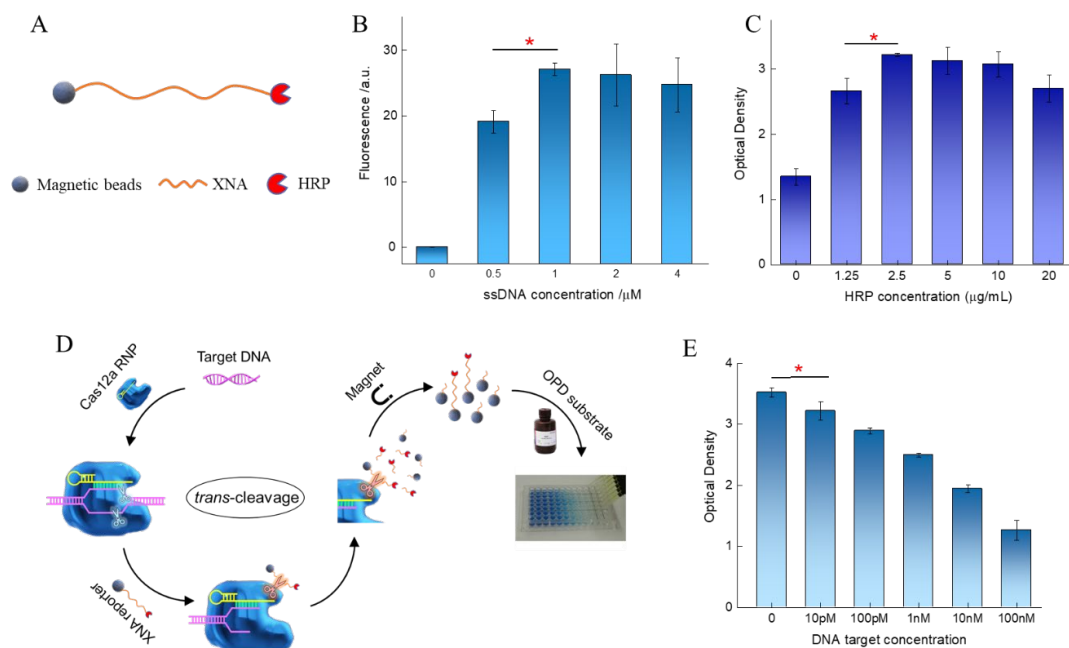


Figure 5. Application of XNA reporter based CRISPR/Cas12a biosensing system for the detection of short synthetic target DNA. (A) Schematic of magnetic beads-XNA-HRP reporter; (B) Optimization of XNA concentration (n=3), and 1 μM is the optimum concentration; (C) Optimization of HRP concentration (n=3), and 2.5 $\mu\text{g/mL}$ is the optimum concentration; (D) Schematic of MB-XNA-HRP reporter based CRISPR/Cas12a biosensing system; (E) Application of MB-XNA-HRP reporter based CRISPR/Cas12a biosensing system for the detection of target DNA. (* $P < 0.05$, ** $P < 0.01$, *** $P < 0.005$, ns = not significant)

Discussion

To date, Cas12a has been found to have varying *trans*-cleavage rates across different types of nucleic acids (ssDNA, dsDNA and ssRNA)¹² and also in response to different nucleobase sequences¹⁴. However, the underlying mechanism remains unclear. In this study, we introduced Xeno nucleic acids (XNA) as *trans*-cleavage substrates for Cas12a to understand the potential mechanism underpinning these differences. To realize different types of XNA, chemical modifications were added to the nucleobases, phosphodiester backbone, or sugar moieties.

To understand the potential mechanism of Cas12a' *trans*-cleavage ability on ssDNA with different nucleobase sequences¹⁴, a range of natural nucleobase sequences and synthetic nucleobase sequences were investigated (Fig. 2). Cas12a's the *trans*-cleavage rates of

Pyrimidine (C and T) were higher than that of Purine (A and G), since the molecular structure of single ring Pyrimidine was simpler than that of two rings Purine. This finding also confirmed by synthetic nucleobase sequences, in which Cas12a's *trans*-cleavage rates of single ring nucleobases (deoxyUridine (dU) and 5-Aza-2'-deoxycytidine) were higher than that of two rings nucleobases (5-Nitroindole and 2-Aminopurine). Therefore, more complex molecular structure of nucleobase was found to reduce the *trans*-cleavage activity of Cas12a. Furthermore, this mechanism may also be applicable to the *trans*-cleavage trends in Cas13a, which also shows higher rates on single ring nucleobases U and C than on double ring nucleobases A and G.²⁴

To understand the potential mechanism of higher Cas12a *trans*-cleavage on ssDNA than ssRNA, various types of modification have been applied on sugar moieties, including 2F-RNA, 2'-O-Methyl, 2-methoxyethyl, and LNA (Fig. 3). Their *trans*-cleavage rates follow the sequence: DNA > 2F-RNA > 2'-O-Methyl > 2-methoxyethyl > LNA, which is consistent with the trend of increasing molecular complexity in 2F-RNA, 2'-O-Methyl, 2-methoxyethyl, and LNA (Fig. 3C). Thus, the complexity of the sugar moiety makes it more difficult for Cas12a to cleave the nucleic acid.

To further explore the *trans*-cleavage ability, backbone modified XNAs were investigated, including beta-L-DNA, phosphorothioate, and azobenzene modifications. Limited fluorescence increases were observed for each, since Cas12a is an endonuclease that cleaves the phosphodiester bond within a polynucleotide chain (DNA or RNA)⁹. Thus, chemical modification on phosphodiester backbone effectively reduces the *trans*-cleavage rate of Cas12a. Additionally, the final *trans*-cleavage rates follow the sequence of beta-L-DNA > phosphorothioate > azobenzene (Fig. 4C), which is consistent with increasing molecular complexity in that sequence (Table S1). We therefore infer that more complex chemical modification on backbone also lead to higher nuclease resistance (Fig. 4B).

In all the three types of chemical modifications, Cas12a demonstrates varying *trans*-cleavage rates, which follow the sequence of nucleobase-modified XNA > sugar moiety-modified XNA > backbone-modified XNA (Table S1). In addition, more complex chemical modifications on either of the three above locations lead to lowering of the *trans*-cleavage activity of Cas12a (Table S1). These findings also apply to a range of Cas12a subtypes (Fig. S2), and comparable *trans*-cleavage performances were observed in both LbCas12a and AsCas12a, demonstrating the universality of observed findings.

Finally, we have shown that nucleobase-modified XNA provides alternative new reporters for CRISPR sensors. In this study, we selected dU modified nucleobase to develop a colorimetric XNA based reporter, which shows excellent biosensing performance for nucleic acid detection with the limit of detection of 10 pM (Fig. 5). In comparison with a typical gold nanoparticle-based colorimetric CRISPR/Cas12a biosensing system, which realizes the limit of detection of 1 nM level without any additional signal amplification technology²⁵, our XNA reporter-based colorimetric CRISPR/Cas12a biosensing system shows a 100 fold improvement of sensitivity since we used HRP for further colorimetric signal amplification.

Conclusion

In this study, we investigated the underlying mechanism of Cas12a's *trans*-cleavage preferences using three types of XNA substrates, which is attributed to varying molecular complexity of different sugar moieties, and nucleobases. Additionally, we found that modulated Cas12a *trans*-cleavage rates were observed on different types of XNAs, with the sequence as follows: nucleobase modified XNA > sugar moieties modified XNA > backbone modified XNA. More complex chemical modifications on either of the three above locations led to lowering of the *trans*-cleavage rate of Cas12a. Finally, an XNA-based colorimetric CRISPR/Cas12a biosensing system was developed for the detection of ctDNA, and its limit of detection was evaluated to be 10 pM with 4 log detection range (10 pM to 100 nM). Therefore, XNA provides a new type of *trans*-cleavage target of Cas12a for sensitive biosensing application in CRISPR based diagnostics area.

Acknowledgements

The authors acknowledge the support of the UNSW SHARP program of E.M. G.

References

- (1) Makarova, K. S.; Haft, D. H.; Barrangou, R.; Brouns, S. J.; Charpentier, E.; Horvath, P.; Moineau, S.; Mojica, F. J.; Wolf, Y. I.; Yakunin, A. F. Evolution and classification of the CRISPR–Cas systems. *Nature Reviews Microbiology* **2011**, *9* (6), 467-477.
- (2) Deng, F.; Li, Y.; Li, B.; Goldys, E. M. Increasing *trans*-cleavage catalytic efficiency of Cas12a and Cas13a with chemical enhancers: Application to amplified nucleic acid detection. *Sensors and Actuators B: Chemical* **2022**, *373*, 132767.
- (3) Deng, F.; Sang, R.; Li, Y.; Deng, W.; Goldys, E. Bifunctional circular DNA amplifier transforms a classic CRISPR/Cas sensor into an ultrasensitive autocatalytic sensor. **2023**.
- (4) Deng, F.; Li, Y.; Qiao, L.; Goldys, E. A CRISPR/Cas12a-assisted on-fibre immunosensor for ultrasensitive small protein detection in complex biological samples. *Analytica Chimica Acta* **2022**, *1192*, 339351.

- (5) Deng, F.; Li, Y.; Hall, T.; Vesey, G.; Goldys, E. M. Bi-functional antibody-CRISPR/Cas12a ribonucleoprotein conjugate for improved immunoassay performance. *Analytica Chimica Acta* **2023**, *1259*, 341211.
- (6) Li, Y.; Deng, F.; Hall, T.; Vesey, G.; Goldys, E. M. CRISPR/Cas12a-powered immunosensor suitable for ultra-sensitive whole *Cryptosporidium* oocyst detection from water samples using a plate reader. *Water Research* **2021**, *203*, 117553.
- (7) Chen, J. S.; Ma, E.; Harrington, L. B.; Da Costa, M.; Tian, X.; Palefsky, J. M.; Doudna, J. A. CRISPR-Cas12a target binding unleashes indiscriminate single-stranded DNase activity. *Science* **2018**, *360* (6387), 436-439.
- (8) Gootenberg, J. S.; Abudayyeh, O. O.; Lee, J. W.; Essletzbichler, P.; Dy, A. J.; Joung, J.; Verdine, V.; Donghia, N.; Daringer, N. M.; Freije, C. A. Nucleic acid detection with CRISPR-Cas13a/C2c2. *Science* **2017**, *356* (6336), 438-442.
- (9) Li, S.-Y.; Cheng, Q.-X.; Wang, J.-M.; Li, X.-Y.; Zhang, Z.-L.; Gao, S.; Cao, R.-B.; Zhao, G.-P.; Wang, J. CRISPR-Cas12a-assisted nucleic acid detection. *Cell discovery* **2018**, *4* (1), 20.
- (10) Swarts, D. C.; Jinek, M. Mechanistic Insights into the cis-and trans-Acting DNase Activities of Cas12a. *Molecular cell* **2019**, *73* (3), 589-600. e584. Li, S.-Y.; Cheng, Q.-X.; Liu, J.-K.; Nie, X.-Q.; Zhao, G.-P.; Wang, J. CRISPR-Cas12a has both cis-and trans-cleavage activities on single-stranded DNA. *Cell research* **2018**, *28* (4), 491-493.
- (11) Mohammad, N.; Talton, L.; Hetzler, Z.; Gongireddy, M.; Wei, Q. Unidirectional trans-cleaving behavior of CRISPR-Cas12a unlocks for an ultrasensitive assay using hybrid DNA reporters containing a 3' toehold. *Nucleic Acids Research* **2023**, gkad715. Yu, H. L.; Cao, Y.; Lu, X.; Hsing, I.-M. Detection of rare variant alleles using the AsCas12a double-stranded DNA trans-cleavage activity. *Biosensors and Bioelectronics* **2021**, *189*, 113382.
- (12) Deng, F.; Li, Y.; Sang, R.; Zhang, C.; Hall, T.; Yang, D.; Goldys, E. RNA reporter based CRISPR/Cas12a biosensing platform for sensitive detection of circulating tumor DNA. In *2023 45th Annual International Conference of the IEEE Engineering in Medicine & Biology Society (EMBC), 2023*; IEEE: pp 1-4. Fuchs, R. T.; Curcuru, J.; Mabuchi, M.; Yourik, P.; Robb, G. B. Cas12a trans-cleavage can be modulated in vitro and is active on ssDNA, dsDNA, and RNA. *BioRxiv* **2019**, 600890.
- (13) Li, J.; Luo, T.; He, Y.; Liu, H.; Deng, Z.; Bu, J.; Long, X.; Zhong, S.; Yang, Y. Discovery of the Rnase activity of CRISPR-Cas12a and its distinguishing cleavage efficiency on various substrates. *Chemical Communications* **2022**, *58* (15), 2540-2543.
- (14) Gong, J.; Kan, L.; Zhang, X.; He, Y.; Pan, J.; Zhao, L.; Li, Q.; Liu, M.; Tian, J.; Lin, S. An enhanced method for nucleic acid detection with CRISPR-Cas12a using phosphorothioate modified primers and optimized gold-nanoparticle strip. *Bioactive materials* **2021**, *6* (12), 4580-4590.
- (15) Lv, H.; Wang, J.; Zhang, J.; Chen, Y.; Yin, L.; Jin, D.; Gu, D.; Zhao, H.; Xu, Y.; Wang, J. Definition of CRISPR Cas12a trans-cleavage units to facilitate CRISPR diagnostics. *Frontiers in Microbiology* **2021**, *12*, 766464.
- (16) Morihiro, K.; Kasahara, Y.; Obika, S. Biological applications of xeno nucleic acids. *Molecular BioSystems* **2017**, *13* (2), 235-245.
- (17) Tu, T.; Huan, S.; Ke, G.; Zhang, X. Functional xeno nucleic acids for biomedical application. *Chemical research in Chinese universities* **2022**, *38* (4), 912-918.
- (18) Pinheiro, V. B.; Holliger, P. Towards XNA nanotechnology: new materials from synthetic genetic polymers. *Trends in biotechnology* **2014**, *32* (6), 321-328.
- (19) Li, B.; Zeng, C.; Li, W.; Zhang, X.; Luo, X.; Zhao, W.; Zhang, C.; Dong, Y. Synthetic oligonucleotides inhibit CRISPR-Cpf1-mediated genome editing. *Cell reports* **2018**, *25* (12), 3262-3272. e3263.
- (20) Ke, Y.; Ghalandari, B.; Huang, S.; Li, S.; Huang, C.; Zhi, X.; Cui, D.; Ding, X. 2'-O-Methyl modified guide RNA promotes the single nucleotide polymorphism (SNP) discrimination ability of CRISPR-Cas12a systems. *Chemical Science* **2022**, *13* (7), 2050-2061.
- (21) McMahon, M. A.; Prakash, T. P.; Cleveland, D. W.; Bennett, C. F.; Rahdar, M. Chemically modified Cpf1-CRISPR RNAs mediate efficient genome editing in mammalian cells. *Molecular Therapy* **2018**, *26* (5), 1228-1240.

- (22) Stejskal, P.; Goodarzi, H.; Srovnal, J.; Hajdúch, M.; van't Veer, L. J.; Magbanua, M. J. M. Circulating tumor nucleic acids: biology, release mechanisms, and clinical relevance. *Molecular Cancer* **2023**, *22* (1), 1-21.
- (23) Hauser, N. C.; Martinez, R.; Jacob, A.; Rupp, S.; Hoheisel, J. D.; Matysiak, S. Utilising the left-helical conformation of L-DNA for analysing different marker types on a single universal microarray platform. *Nucleic acids research* **2006**, *34* (18), 5101-5111.
- (24) Gootenberg, J. S.; Abudayyeh, O. O.; Kellner, M. J.; Joung, J.; Collins, J. J.; Zhang, F. Multiplexed and portable nucleic acid detection platform with Cas13, Cas12a, and Csm6. *Science* **2018**, *360* (6387), 439-444.
- (25) Hu, M.; Yuan, C.; Tian, T.; Wang, X.; Sun, J.; Xiong, E.; Zhou, X. Single-step, salt-aging-free, and thiol-free freezing construction of AuNP-based bioprobes for advancing CRISPR-based diagnostics. *Journal of the American Chemical Society* **2020**, *142* (16), 7506-7513. Li, Y.; Mansour, H.; Wang, T.; Poojari, S.; Li, F. Naked-eye detection of grapevine red-blotch viral infection using a plasmonic CRISPR Cas12a assay. *Analytical Chemistry* **2019**, *91* (18), 11510-11513.